SOILS AND FOUNDATIONS Vol. 50, No. 3, 421–429, June 2010
Japanese Geotechnical Society

COMPARISON OF LIQUEFACTION-INDUCED GROUND DEFORMATION BETWEEN RESULTS FROM UNDRAINED CYCLIC TORSIONAL SHEAR TESTS AND OBSERVATIONS FROM PREVIOUS MODEL TESTS AND CASE STUDIES

Takashi Kiyota[i], Junichi Koseki[ii] and Takeshi Sato[iii]

ABSTRACT

In order to investigate liquefaction-induced ground displacement, we conducted a series of undrained cyclic torsional shear tests on saturated Toyoura sand using a modified torsional apparatus capable of applying and measuring double amplitude shear strain up to about 100%. The limiting value of double amplitude shear strain, at which strain localization appears during undrained cyclic loading tests, was evaluated from the test results with reference to the change in the deviator stress during liquefaction. The limiting strain values, which increase with a decrease in the relative density of the specimen, were found to be consistent with the maximum amounts of liquefaction-induced ground displacement observed in the previous shaking table model tests and most of the relevant case studies. This feature is reasonable considering the reduction in the mobilized cyclic shear stress in liquefied soil due to the degradation of the shear resistance. As long as the liquefied soil layer remains in uniform deformation, these limiting strain values may be used in estimating the maximum amount of liquefaction-induced ground displacement.

Key words: case study, lateral flow, liquefaction, model test, sandy soil, torsional shear (**IGC**: D6)

INTRODUCTION

Large ground deformation caused by liquefaction has been observed during past earthquakes, resulting in serious damage to structures, including harbor facilities and underground structures. For example, liquefaction-induced ground displacement during the 1964 Niigata earthquake reached several meters as reported by Hamada et al. (1988). The occurrence of large ground deformation in the reclaimed areas behind the quay walls during the 1995 Hyogoken-Nanbu earthquake was also caused by liquefaction (e.g., Hamada et al., 1996; Ishihara et al., 1996). In order to reveal such liquefaction-induced large ground deformation, significant experimental and theoretical research works have been carried out. However, the development of an accurate but practical method for estimating liquefaction-induced ground deformation is still an important task in earthquake geotechnical engineering.

Since conventional laboratory tests have technical difficulty in investigating the large strain properties of liquefied soils, model tests have been carried out by many researchers (e.g., Yasuda et al., 1992; PWRI, 1989). They observed that the large displacements are associated with strains induced in the liquefied ground in the order of several tens of percent or even larger. Based on a series of model tests, Sasaki et al. (1992) suggested that the gravity force is highly influential on the event of the liquefied ground movement, which was also evident from case studies conducted by Hamada et al. (1988) among others. In addition, Kokusho (2000) reported that significant deformation could be associated not only with the driving force due to the gravity but also a formation of a water film in the liquefied layer.

In order to investigate the above large strain liquefaction properties, we modified a torsional shear apparatus and performed a series of undrained cyclic torsional shear tests up to a double amplitude shear strain of about 100% (Kiyota et al., 2008). We found that there is a limiting value of double amplitude shear strain, $\gamma_{L(DA)}$, to initiate strain localization.

In this study, with respect to liquefaction-induced large ground displacement, the outline of the above torsional shear tests results is first presented, and then the values of $\gamma_{L(DA)}$ and the amounts of permanent ground displacement that were observed from previous shaking table model tests and case studies (1923 Kanto earthquake, 1948 Fukui earthquake, 1964 Niigata earthquake and 1995 Hyogo-ken Nambu earthquake) are compared.

[i] Associate Professor, Institute of Industrial Science, University of Tokyo, Japan (kiyota@iis.u-tokyo.ac.jp).
[ii] Professor, ditto.
[iii] Professional General Manager, Integrated Geotechnology Institute Limited, Japan.
The manuscript for this paper was received for review on August 31, 2009; approved on April 5, 2010.
Written discussions on this paper should be submitted before January 1, 2011 to the Japanese Geotechnical Society, 4-38-2, Sengoku, Bunkyo-ku, Tokyo 112-0011, Japan. Upon request the closing date may be extended one month.

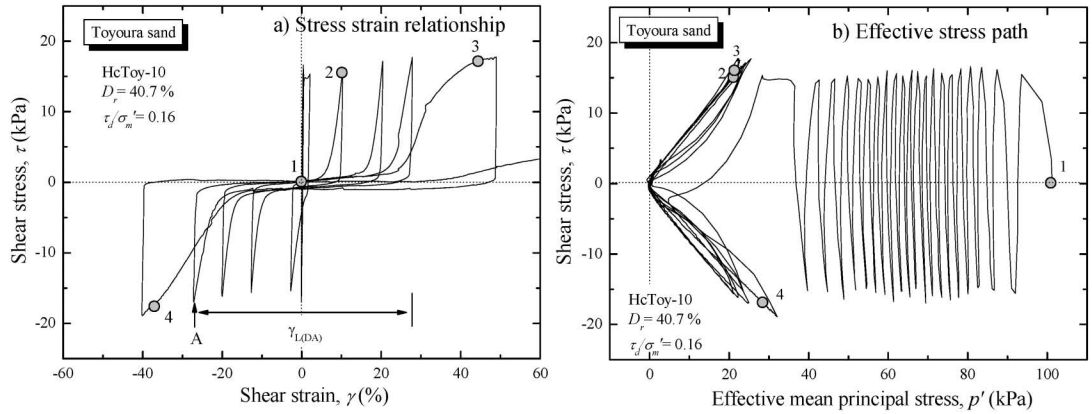

Fig. 1. Typical test result of Toyoura sand (D_r = 40.7%)

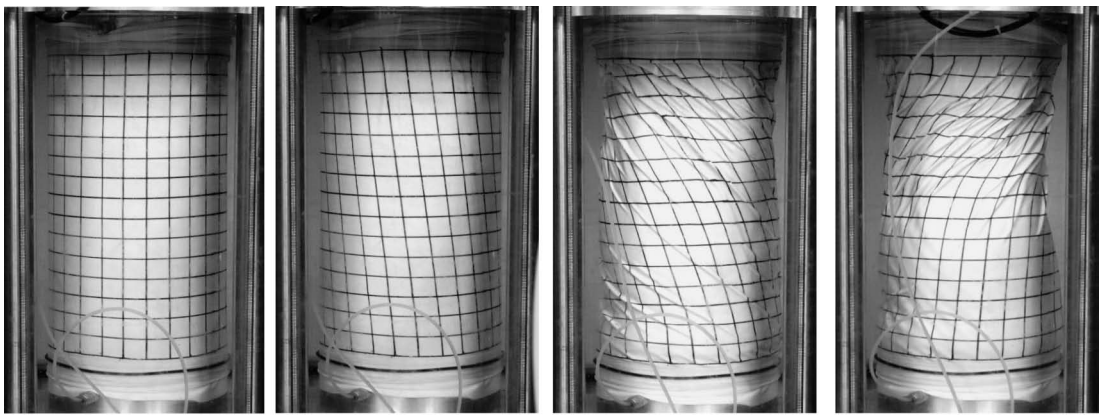

a) State 1. Before test b) State 2. γ= 10 % c) State 3. γ= 40 % d) State 4. γ= -36 %

Photo 1. Specimen deformation at states 1 through 4 in Fig. 1

LIMITING VALUE OF SHAER STRAIN TO INITIATE STRAIN LOCALIZATION

Details of the hollow cylindrical torsional shear apparatus and the tested materials have already been described by Kiyota et al. (2008). Thus, only the results from undrained cyclic torsional shear tests (referred to as large strain liquefaction tests herein) on isotropically consolidated specimens will be briefly shown here. It should be noted that during the liquefaction tests in the present study, the specimen height was kept constant.

A typical test result on a medium loose specimen of saturated Toyoura sand with a relative density, D_r, of approximately 40% is shown in Fig. 1. As the number of cycles was increased, a decrease in the effective stress was observed, and it was accompanied by a significant development of double amplitude shear strain, $\gamma_{(DA)}$. As shown in the stress-strain relationship after state 2 in Fig. 1(a), the increment in the shear strain, $\Delta\gamma$, induced at the time intervals when the effective stress became almost zero increased significantly, and the value of $\gamma_{(DA)}$ amounted to more than 80% at state 4, as shown in Fig. 1(a), while cyclic mobility was observed, as seen in Fig. 1(b).

The specimen deformation at several states, numbered 1 through 4 in Fig. 1, is shown in Photo 1. At state 2 with shear strain, γ of about 10%, the deformation was rather uniform except for the regions near the top cap and the pedestal affected by the end restraint. At state 3, with a γ value of about 40%, the outer membrane wrinkled at several locations. At state 4, with a γ value of about −36%, the concentration of the deformation in the upper part of the specimen was enhanced. In all of these large strain liquefaction tests, the $\gamma_{(DA)}$ values continued to increase and approached almost 100%, that is, the capacity of the apparatus, irrespective of specimen densities. However, non-uniform deformation or strain localization was observed at large strain levels, as shown in Photo 1(d). Refer to Kiyota et al. (2008) for the other test results with which the relative densities and the applied cyclic stress ratios, τ_d/σ'_m, differ from those shown in Fig. 1 and Photo 1.

From the liquefaction test results, the residual deformation of the liquefied specimen was found to consist of two modes of deformation. One is uniform deformation, and the other is non-uniform deformation associated with the strain localization. However, the initiation of strain localization could not be clearly defined based only

on visual observations of specimen deformation.

Meanwhile, Tatsuoka et al. (1986) performed drained torsional shear tests and reported that vertical strain, which decreased due to positive dilatancy with straining, started to increase when the shear band was formed. This phenomenon caused a decrease in the q ($=\sigma'_v-\sigma'_h$) value during undrained cyclic torsional shear loading while keeping the specimen height constant.

Figure 2 shows a time history of the q value during the liquefaction test on Toyoura sand, as was shown in Fig. 1. The amplitude of the cyclic change in q decreased suddenly at state A. Such sudden change of the q value is possibly linked with the formation of shear bands and thus with strain localization. Based on this observation, the limiting value of double amplitude shear strain, $\gamma_{L(DA)}$, to initiate strain localization was defined based on the last cycle data when the limiting state appeared (*see* state A in Figs. 1(a) and 2).

As a result, the $\gamma_{L(DA)}$ value was found to increase with a decrease in the D_r value of the specimen for Toyoura sand, as shown in Fig. 3. In addition, Kiyota et al. (2008) showed that the values of $\gamma_{L(DA)}/2$ of Toyoura sand could be linked to the empirical relationships among the cyclic shear stress ratio, the maximum possible shear strain and

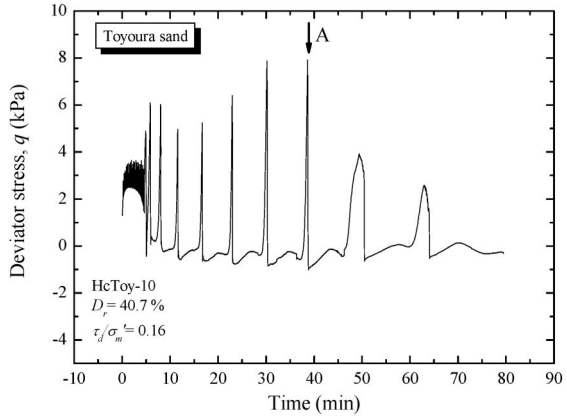

Fig. 2. Time history of deviator stress (cf. Fig. 1)

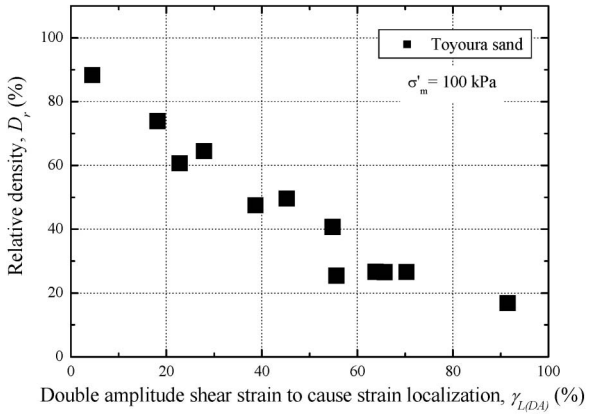

Fig. 3 Relationship between $\gamma_{L(DA)}$ and D_r (modified after Kiyota et al., 2008)

the adjusted SPT-N value, which were presented by Tokimatsu and Asaka (1998).

COMPARISON OF $\gamma_{L(DA)}$ VALUES AND RESULTS FROM PREVIOUS MODEL TESTS AND CASE STUDIES

From the observation of large strain liquefaction tests, the deformation mode of liquefied soil was found to shift from uniform to non-uniform deformation. The latter deformation mode is associated with strain localization. In addition, the limiting values of shear strain to initiate strain localization, $\gamma_{L(DA)}$, were evaluated. As far as the authors know, however, there is no report where the localization of liquefied soil is observed. Therefore, the value of $\gamma_{L(DA)}$ may be linked with the maximum shear strain of the liquefied layer, and an attempt was made to compare the $\gamma_{L(DA)}$ values and results from previous model tests and case studies.

Figures 4 and 5 show the liquefaction-induced ground displacement measured by previous model tests and case studies, respectively, as summarized in Tables 1 and 2. For comparison, the $\gamma_{L(DA)}/2$ values of Toyoura sand obtained by Kiyota et al. (2008) are also shown in these figures. For reference, Figs. 6, 7 and 8 show the model types and the typical results of model tests performed by Yasuda et al. (1992) and PWRI (1989), while Fig. 9 shows the types of cross-section in the case studies. By referring to Meyerhof (1957), the D_r value of possibly liquefied soil in the case studies was evaluated using the relationship between D_r and the averaged SPT-N value, N, as follows;

$$D_r = 21\sqrt{\frac{N}{\frac{\sigma'_z}{98}+0.7}}\ (\%) \qquad (1)$$

in which σ'_z denotes the effective vertical stress in kPa.

It should be noted that the limiting value of shear strain, as indicated in Figs. 4 and 5, was set to half the value of $\gamma_{L(DA)}$, because $\gamma_{L(DA)}$ in this study were defined as double amplitude shear strain while the displacement measured in the model tests and case studies was based on a single amplitude. The tested materials in the model tests shown in Fig. 4 and Table 1 were fine sands, as summarized in Fig. 10, and are similar to Toyoura sand. The liquefiable deposits observed in the case studies for the 1923 Kanto earthquake, the 1948 Fukui earthquake and the 1964 Niigata earthquake consisted of sandy soils, while the liquefied fill during 1995 Hyogo-ken Nambu earthquake was mainly composed of Masado, a weathered granite that had been excavated from the Rokko Mountains and Awaji Island.

Note also that, in Figs. 4 and 5, the shear strain of the liquefied ground in the model tests and case studies was defined as D/H, where D is the horizontal displacement at the top of the ground surface or local horizontal displacement in the liquefied layer, as was reported by each of the previous studies, and H is the thickness of the liquefied layer, as shown in Figs. 6 and 9. The value of H for sloped ground was estimated from the information

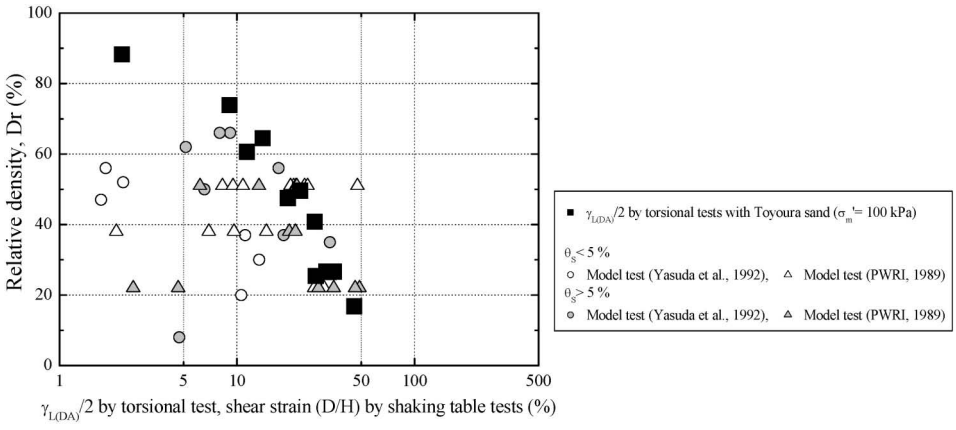

Fig. 4. Comparison between $\gamma_{L(DA)}/2$ and results from model tests

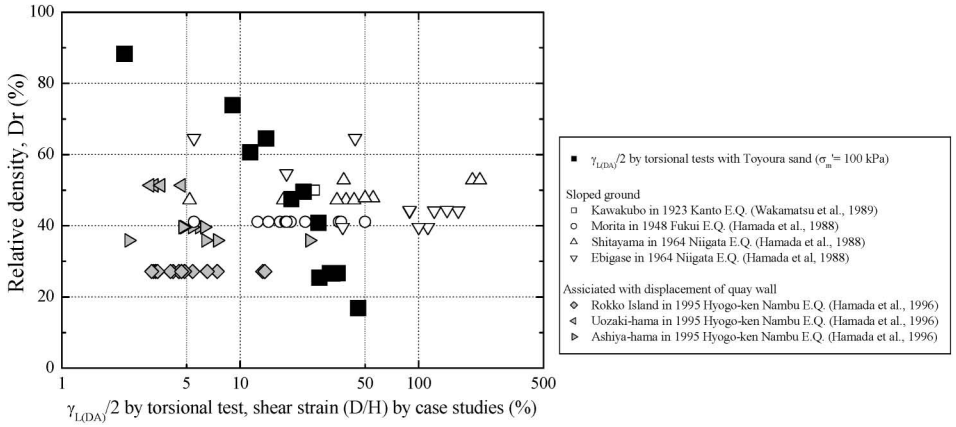

Fig. 5. Comparison between $\gamma_{L(DA)}/2$ and results from case studies

provided in each of the case studies as shown in Fig. 9(a). On the other hand, the value of H for the reclaimed land areas behind the quay wall was set to be the thickness of the reclaimed soil, as shown in Fig. 9(b).

It is likely that the usage of D/H corresponding to a simple shear mode like the shear strain induced in the liquefied soil layer leads to a rough estimation. Sasaki et al. (1992) and Towhata et al. (1992) pointed out that the distribution of the displacement of liquefied ground can be approximated by a sinusoidal curve. Under such approximation, the maximum shear strain would be $\pi/2$ times as large as the shear strain, D/H, evaluated under the assumption of simple shear deformation. However, the difference in the shear strains by a factor of $\pi/2$ would not be significant when they are plotted on a logarithmic scale. In addition, the actual deformation mode may not be always unique, as can be seen in the observations from the previous model tests (Figs. 7 and 8). Therefore, we adopted the D/H value in this study in order to simplify the evaluation procedure.

The slope of the ground surface and the slope of the bottom of the liquefied layer in the model tests varied between 0 to 10%, while those in the case studies were reported as gentle slopes (e.g., less than 1% for Ebigase in 1964 Niigata earthquake). In addition, the liquefied fill during 1995 Hyogo-ken Nambu earthquake was located behind the quay wall that suffered damage involving outward residual displacement.

The amount of D/H observed in the model tests seems to depend not only on the slope of the ground surface, θ_S, but also on that of the bottom of the liquefied layer, θ_B, as shown in Fig. 4 and Table 1. On the other hand, the D/H value evaluated for the case studies associated with the displacement of quay wall was relatively small compared with that of the sloped ground, as shown in Fig. 5. As a whole, the $\gamma_{L(DA)}/2$ values seem to be consistent in general with the maximum value of liquefaction-induced residual shear strain measured by previous model tests and case studies, except for the cases for the sloped ground in the 1964 Niigata earthquake reported by Hamada et al. (1988) that were significantly larger than the $\gamma_{L(DA)}/2$ values.

DISCUSSIONS

To understand the above correlation between $\gamma_{L(DA)}/2$ and the residual deformation by the model tests and case studies, the following possible factors could be considered.

Table 1. Reference data of liquefaction-induced ground displacement in model tests used in Fig. 4

data	Type of sand*	Base acceleration (gal)	θ_S^* (%)	θ_B^* (%)	H′* (cm)	H* (cm)	D* (cm)	γ=D/H (%)	D_r (%)	References
A-1	S	300	0	5	17.5	17.5	0.3	1.7	47	Yasuda et al. (1992)
A-2	S	300	0	10	17.5	17.5	0.4	2.3	52	Yasuda et al. (1992)
A-4	S	300	0	5	27.5	27.5	0.5	1.8	56	Yasuda et al. (1992)
B-1	S	300	5	5	17.5	17.5	1.6	9.1	66	Yasuda et al. (1992)
B-2	S	300	10	10	17.5	17.5	3	17.1	56	Yasuda et al. (1992)
B-3	S	300	5	5	7.5	7.5	0.6	8	66	Yasuda et al. (1992)
B-4	S	300	5	5	27.5	27.5	1.8	6.5	50	Yasuda et al. (1992)
C-1	S-F	300	5	5	17.5	17.5	0.9	5.1	62	Yasuda et al. (1992)
F-1	S	300	5	5	27.5	27.5	1.3	4.7	8	Yasuda et al. (1992)
G-1	TS	300	0	5	18	18	2	11.1	37	Yasuda et al. (1992)
G-2	TS	300	0	10	18	18	2.4	13.3	30	Yasuda et al. (1992)
G-3	TS	300	5	5	18	18	3.3	18.3	37	Yasuda et al. (1992)
G-4	TS	300	10	10	18	18	6	33.3	35	Yasuda et al. (1992)
H-1	TS	300	0	5	18	18	1.9	10.6	20	Yasuda et al. (1992)
1-1-B	SS	85.4	5	0	70	40	5.31	13.3	51	PWRI (1989)
1-1-C	SS	85.4	5	0	70	40	2.47	6.2	51	PWRI (1989)
1-2-B	SS	120.6	5.1	0	70	40	8.61	21.5	51	PWRI (1989)
1-2-C	SS	120.6	5.1	0	70	40	8.69	21.7	51	PWRI (1989)
1-3-B	SS	166.6	4.1	0	70	40	8.34	20.8	51	PWRI (1989)
1-3-C	SS	166.6	4.1	0	70	40	9.61	24.0	51	PWRI (1989)
1-4-B	SS	223.0	3.8	0	70	40	3.31	8.3	51	PWRI (1989)
1-4-C	SS	223.0	3.8	0	70	40	3.80	9.5	51	PWRI (1989)
2-1-B	SS	167.5	7.4	0	35	20	0.93	4.7	22	PWRI (1989)
2-1-C	SS	167.5	7.4	0	35	20	0.52	2.6	22	PWRI (1989)
2-2-B	SS	128.3	7.4	0	35	20	5.75	28.7	22	PWRI (1989)
2-2-C	SS	128.3	7.4	0	35	20	7.02	35.1	22	PWRI (1989)
2-3-B	SS	168.6	6.4	0	35	20	9.80	49.0	22	PWRI (1989)
2-3-C	SS	168.6	6.4	0	35	20	9.26	46.3	22	PWRI (1989)
2-4-B	SS	129.5	4.8	0	35	20	5.44	27.2	22	PWRI (1989)
2-4-C	SS	129.5	4.8	0	35	20	6.18	30.9	22	PWRI (1989)
3-1-B	SS	159.2	4.7	5	19	10	2.50	25.0	51	PWRI (1989)
3-1-C	SS	159.2	4.7	5	13	10	1.33	13.3	51	PWRI (1989)
3-2-B	SS	163.2	4.9	5	19	10	4.77	47.7	51	PWRI (1989)
3-2-C	SS	163.2	4.9	5	13	10	2.00	20.0	51	PWRI (1989)
3-3-B	SS	137.5	4.9	5	19	10	1.08	10.8	51	PWRI (1989)
4-2-B	SS	119.5	4.7	0	35	20	2.93	14.7	38	PWRI (1989)
4-2-C	SS	119.5	4.7	0	35	20	1.39	6.9	38	PWRI (1989)
4-3-B	SS	158.8	5.7	0	35	20	3.94	19.7	38	PWRI (1989)
4-3-C	SS	158.8	5.7	0	35	20	4.27	21.3	38	PWRI (1989)
4-4-B	SS	203.4	4.8	0	35	20	0.42	2.1	38	PWRI (1989)
4-4-C	SS	203.4	4.8	0	35	20	1.92	9.6	38	PWRI (1989)

S: clean sand, S-F: sand with fines, TS: Toyoura sand, SS: Sengenyama sand
θ_S: slope of the ground surface, θ_B: slope of the bottom of the liquefied layer
H′: thickness of the liquefied layer at the measured point
H: thickness of the liquefied layer for the calculation of γ
D: displacement on the ground surface or local deformation of the liquefied layer

Table 2. Reference data of liquefaction-induced ground displacement in case studies used in Fig. 5

Event	Location	Geology of liquefied sand	Type of deformation*	Number of data used	H* (m)	D* (m)	$\gamma = D/H$ (%)	SPT-N value	Ave. D_r (%)	References
1923 Kanto E.Q.	Kawakubo	Alluvial sand	S	1	5.75	1.5	26.1	1–16	50	Wakamatsu et al. (1989)
1948 Fukui E.Q.	Morita	Alluvial sand	S	11	4.3–8.6	0.5–3.3	5.6–50	1–10	41	Hamada et al. (1988)
1965 Niigata E.Q.	Shitayama	Alluvial sand	S	11	2.8–6.4	0.3–6.1	5.2–220	3–12	47–53	Hamada et al. (1988)
	Ebigase	Alluvial sand	S	13	3.8–5.2	0.2–7.1	5.5–166	0–17	39–64	Hamada et al. (1988)
1995 Hyogoken-Nambu E.Q.	Rokko Island	Rokko granite, Kobe group, Osaka group	Q	15	14–16	0.5–2.4	3.2–17.1	1–6	27	Hamada et al. (1996)
	Uozaki-hama	Rokko granite	Q	4	11.8–12.8	0.4–1.0	3.1–8.4	2–30	51–52	Hamada et al. (1996)
	Ashiya-hama	Marine sand, Ruoke granite	Q	9	9.7–11.6	0.2–2.6	2.4–24.4	0–23	36–40	Hamada et al. (1996)

S: deformation on the slope ground
Q: deformation associated with displacement of quay wall
H: thickness of the estimated liquefied layer at the measured point
D: displacement on the ground surface

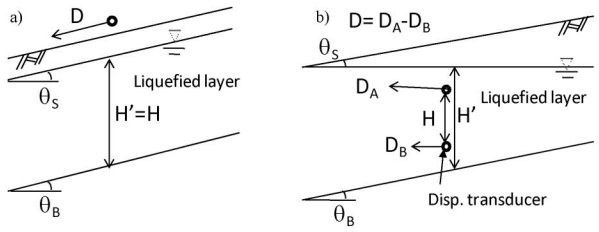

Fig. 6. Model types employed by a) Yasuda et al. (1992) and b) PWRI (1989) (cf. Fig. 4)

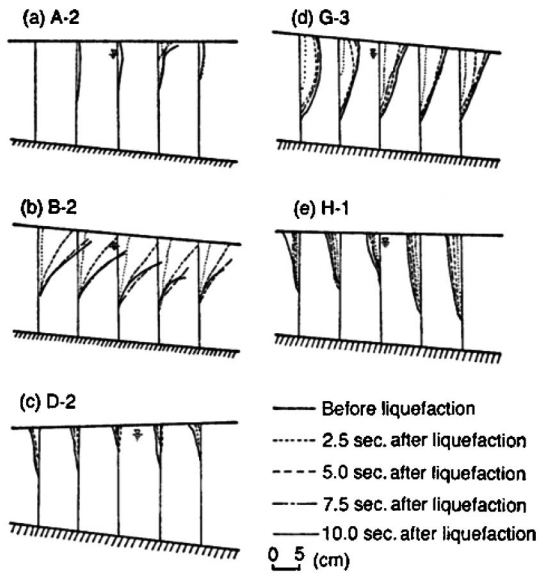

Fig. 7. Typical observation in model test (Yasuda et al., 1992)

Degradation of Shear Resistance

Elgamal et al. (1997) showed that the mobilized cyclic shear stress in the liquefied soil reduced due to the degradation of the shear resistance. They were able to back-calculate the degradation from the acceleration record from case histories (*see* Fig. 11). In fact, PWRI (1989) among others reported that the response of the accelerometers that were set on the liquefied layer in the model became smaller during shaking. Sasaki et al. (1992) reported that liquefied sand undergoing lateral displacement behaves in a similar manner to a liquid that exhibits no shear resistance.

When considering the effects of the degradation of shear resistance during the liquefaction process caused by actual earthquake motions with a limited number of cycles, earthquake-induced shear stress should not be transferred through the liquefied layer. Yet, such a base isolation effect in the actual liquefied ground during the 1987 Superstition Hills earthquake in the US was reported by Youd et al. (1988)

Unlike the above actual behaviour of liquefied soil, the amplitude of cyclic shear stress in the large strain liquefaction tests was kept constant until the end of cyclic loading. The deformation of the specimen was not terminated until the double amplitude shear strain, $\gamma_{(DA)}$, reached about 100%, that is, the full capacity of the apparatus. Therefore, the effects of the degradation of shear resistance during the liquefaction process could not be observed directly.

Instead, as typically shown in Fig. 12, strain softening behaviour associated with degradation of shear resistance could be observed in the relationships between the shear strain and modified shear stress ratio, $(\tau - \Delta\tau)/(p' + \Delta p')$. The modified shear stress ratio was adopted in order to correct the effects of the mobilization of shear resistance under extremely low effective stress states and possible measurement error. Refer to Koseki et al. (2005) for the details of the modified shear stress ratio. Kiyota et al. (2008) pointed out that the above strain softening cor-

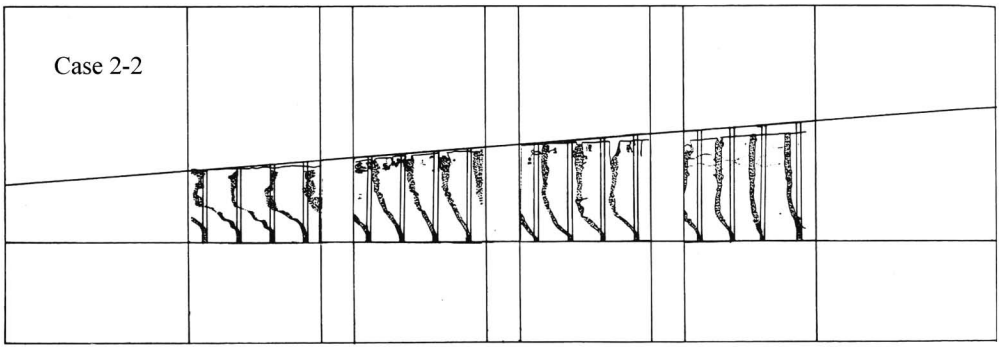

Fig. 8. Typical observation in model test (PWRI, 1989)

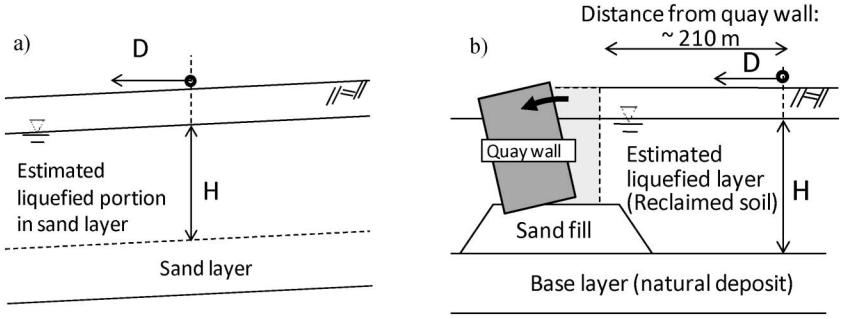

Fig. 9 Schematic cross-sections in case studies on a) slope ground (Wakamatsu et al., 1989; Hamada et al., 1988) and b) ground behind quay wall (Hamada et al., 1996) (cf. Fig. 5)

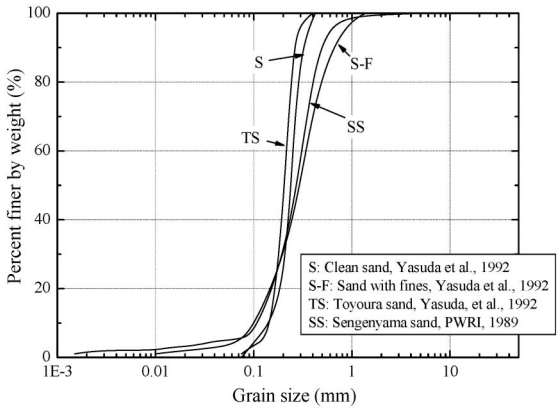

Fig. 10. Grain size distribution curves of sands used in Fig. 4

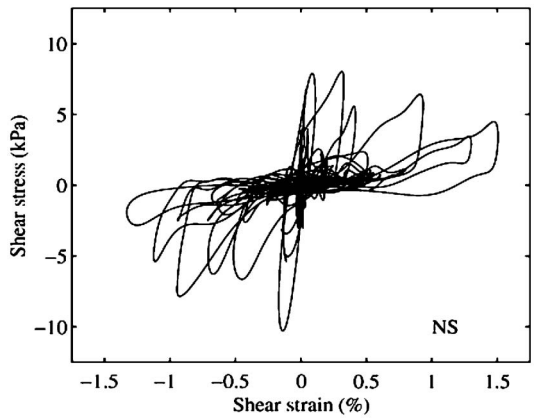

Fig. 11 N-S shear stress-strain relationship during the 1987 Superstition Hills earthquake evaluated from acceleration histories (Elgamal et al., 1997)

responds to the strain localization as well as the $\gamma_{L(DA)}$, as shown in Fig. 12.

Influence of Gravity Force

Case histories that were investigated by aerial photo surveys at the areas where liquefaction occurred indicate that the ground deformation of gentle slopes is oriented from higher elevations toward lower ones (Hamada et al., 1989; Yasuda et al., 1989; Wakamatsu et al., 1989; O'Rourke et al., 1989), while that of reclaimed islands occurs toward the sea, as was the case with the residual displacement of the quay wall (Hamada et al., 1996). Their studies suggest that the gravity force is highly influential on the event of the liquefied ground movement. It should be noted that Sasaki et al. (1992) performed model tests where the model ground was shaken in both perpendicular and parallel direction to the sloped ground. As a result, the deformation vector of the ground surface was independent of the direction of the excitation, and was shown to depend solely on the direction of the slope. They reported, therefore, that the gravity force is the agent controlling the liquefaction-induced ground displacement, while the effects of an inertia force of liquefied soil are insignificant.

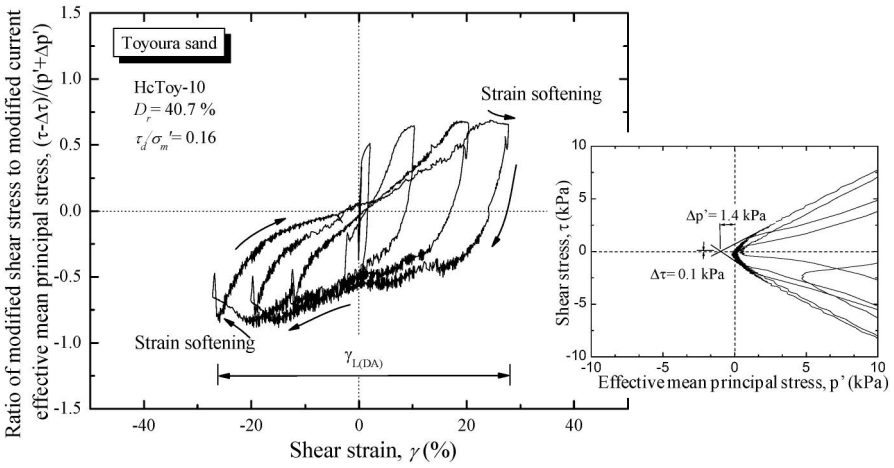

Fig. 12 Relationships between shear stress ratio and shear strain with correction (cf. Fig. 1)

In view of the above, the deformation of liquefied soil develops by the gravity force during and after the ground shaking, and the strain localization develops when the deformation exceeds the $\gamma_{L(DA)}/2$ value. The maximum deformation of liquefied soil in the model tests and case studies corresponded to the $\gamma_{L(DA)}/2$ value in general, as shown in Figs. 4 and 5. The results suggest that, for the model tests and case studies with gentle slopes of ground surface, the effect of gravity force mobilized in the liquefied layer was not large enough to develop strain localization. Likewise, Yasuda et al. (1992) reported that the liquefied layer in their model tests deformed without any strain localization as shown in Fig. 7. In addition, the result from the model test conducted by PWRI (1989) also revealed that the liquefaction-induced ground deformation was associated with almost uniform deformation as shown in Fig. 8. Note that it might be difficult to detect the strain localization accurately in the model tests conducted by Yasuda et al. (1992) because they used noodles for the deformation measurement.

It is likely that the deformation of liquefied ground with steep slopes would exceed the $\gamma_{L(DA)}/2$ value. In this case, we should take into account the deformation characteristics after strain localization to reasonably estimate the maximum ground deformation.

Other Influential Factors

The residual shear strains in the 1964 Niigata earthquake were significantly larger than the value of $\gamma_{L(DA)}$, as shown in Fig. 5, and we have no concrete reason for this. Since it is impossible to estimate accurately the actual thickness of the liquefied layer, H, in case studies, it is possible that the value of H was underestimated, resulting in the overestimation of the residual shear strain, γ.

On the other hand, it should be noted that the $\gamma_{L(DA)}$ value presented in this study is associated only with the undrained condition. When the excess pore water pressure is dissipated during each shaking or the time intervals between the main-shock and after-shocks, the value of $\gamma_{L(DA)}$ may be affected by such dissipation history.

The $\gamma_{L(DA)}$ value could be affected by stress histories as well as initial static shear stress. The authors began conducting experiments to consider these problems.

In addition, when the liquefied layer is overlain by a soil with lower permeability, the void redistribution may cause a so-called water film effect (Kokusho, 1999) since the liquefied layer expels a certain volume of pore water as it densifies. This could be a trigger of large displacement with strain localization during and after earthquakes (e.g., Kokusho, 2000; Malvick et al., 2008). In fact, Kokusho (2000) reported that considerable displacement of sandy ground including several silty sub-layers took place in the Hakusan District during the 1964 Niigata earthquake. However, since our discussion on the mechanism of liquefaction-induced ground deformation is based on the experiments on homogeneous sandy samples, behavior affected by a difference in the permeabilities of layered silt and sand is beyond the scope of this paper.

As mentioned above, there are several issues that are left to be clarified in comparing the liquefaction-induced ground deformation between results from laboratory tests and observations from case studies.

On the other hand, the $\gamma_{L(DA)}$ values evaluated in the laboratory test were consistent with the results from the model tests that were conducted under controlled testing conditions, such as the thickness of the liquefied layer.

CONCLUSIONS

In the present study, attempts were made to investigate the relationships between the limiting values of double amplitude shear strain, $\gamma_{L(DA)}$, to initiate strain localization that were evaluated based on the large strain undrained cyclic torsional shear tests on sand, and the results from previous model tests and case studies.

From the above comparisons, it was found that there is a certain correlation between the $\gamma_{L(DA)}/2$ values by torsional shear tests and the maximum values of shear strain obtained by the shaking table model tests and most of the case studies. For example, at a relative density, D_r, of about 60 to 80%, they are about 10%, while at D_r of

about 20 to 40%, they are about 30%.

The above correlation between the $\gamma_{L(DA)}/2$ values and the results from model tests and case studies suggests that the strain localization did not develop during or after ground shaking, due possibly to degradation of the shear resistance of the liquefied layer and the influence of the gravity force that was not large enough to induce the strain localization in the liquefied layer.

Under the condition that strain localization does not develop, these $\gamma_{L(DA)}$ values may be used in estimating the maximum amount of liquefaction-induced ground displacement.

Further research is required on the conditions under which the strain localization of liquefied soil occurs, as well as the specific factors which influence it.

REFERENCES

1) Elgamal, A. W., Zeghal, M. and Parra, E. (1997): Identification and modelling of earthquake response, *1st Int. Conf. on Earthquake Geotechnical Engineering, IS-Tokyo '95*, **3**, 1369–1406.
2) Hamada, M., Yasuda, S. and Wakamatsu, K. (1988): Case studies on liquefaction-induced permanent ground displacement, *Proc. 1st JAPAN-U.S. Workshop on Liquefaction, Large Ground Deformation and Their Effects on Lifeline Facilities*, 3–21.
3) Hamada, M., Wakamatsu, K. and Yasuda, S. (1989): Liquefaction-induced ground displacement during the 1948 Fukui earthquake, *Proc. 2nd US-JAPAN Workshop on Liquefaction, Large Ground Deformation and Their Effects on Lifelines*, 6–15.
4) Hamada, M., Isoyama, R. and Wakamatsu, K. (1996): Liquefaction-induced ground displacement and its related damage to lifeline facilities, *Soils and Foundations, Special Issue on Geotechnical Aspects of the January 17 1995 Hyogoken-Nambu Earthquake*, 81–97.
5) Ishihara, K., Yasuda, S. and Nagase, H. (1996): Soil characteristics and ground damage, *Soils and Foundations, Special Issue on Geotechnical Aspects of the January 17 1995 Hyogoken-Nambu Earthquake*, 109–118.
6) Kiyota, T., Sato, T., Koseki, J. and Abadimarand, M. (2008): Behavior of liquefied sands under extremely large strain levels in cyclic torsional shear tests, *Soils and Foundations*, **48**(5), 727–739.
7) Kokusho, T. (1999): Formation of water film in liquefied sand and its effect on lateral spread, *J. Geotech. Geoenvironment Engineering*, ASCE, **125**(10), 817–826.
8) Kokusho, T. (2000): Mechanism for water film generation and lateral flow in liquefied sand layer, *Soils and Foundations*, **40**(5), 99–111.
9) Koseki, J., Yoshida, T. and Sato, T. (2005): Liquefaction properties of Toyoura sand in cyclic torsional shear tests under low confining stress, *Soils and Foundations*, **45**(5), 103–113.
10) Malvick, E. J., Kutter, B. L. and Boulanger, R. W. (2008): Postshaking shear strain localization in a centrifuge model of a saturated sand slope, *Journal of Geotechnical and Geoenvironmental Engineering*, **134**(2), 164–174.
11) Meyerhof, G. G. (1957): Discussion, *Proc. 4th ICSMFE*, **3**, 110.
12) O'Rourke, T. D., Roth, B. L. and Hamada, M. (1989): A case study of large ground deformation during 1971 San Fernando earthquake, *Proc. 2nd US-JAPAN Workshop on Liquefaction, Large Ground Deformation and Their Effects on Lifelines*, 50–66.
13) Public Works Research Institute (1989): Liquefaction-induced lateral deformation on shaking table model tests, *PWRI Research Report*, No. 2768 (in Japanese).
14) Sasaki, Y., Towhata, I., Tokida, K., Yamada, K., Matsumoto, H., Tamari, Y. and Saya, S. (1992): Mechanism of permanent displacement of ground caused by seismic liquefaction, *Soils and Foundations*, **32**(3), 79–96.
15) Tatsuoka, F., Sonoda, S., Hara, K., Fukushima, S. and Pradhan, T. B. S. (1986): Failure and deformation of sand in torsional shear, *Soils and Foundations*, **26**(4), 79–97.
16) Tokimatsu, K. and Asaka, Y. (1998): Effects of liquefaction-induced ground displacements on pile performance in the 1995 Hyogoken-Nambu earthquake, *Soils and Foundations, Special Issue on Geotechnical Aspects of the January 17 1995 Hyogoken-Nambu Earthquake*, (2), 163–177.
17) Towhata, I., Sasaki, Y., Tokida, K., Matsumoto, H., Tamari, Y. and Yamada, K. (1992): Prediction of permanent displacement of liquefied ground by means of minimum energy principle, *Soils and Foundations*, **32**(3), 97–116.
18) Wakamatsu, K., Hamada, M., Yasuda, S. and Morimoto, I. (1989): Liquefaction induced ground displacement during the 1923 Kanto earthquake, *Proc. 2nd US-JAPAN Workshop on Liquefaction, Large Ground Deformation and Their Effects on Lifelines*, 36–49.
19) Yasuda, S., Hamada, M., Wakamatsu, K. and Morimoto, I. (1989): Liquefaction induced permanent ground displacement in Niigata City, *Proc. 2nd US-JAPAN Workshop on Liquefaction, Large Ground Deformation and Their Effects on Lifelines*, 67–81.
20) Yasuda, S., Nagase, H., Kiku, H. and Uchida, Y. (1992): The mechanism and a simplified procedure for the analysis of permanent ground displacement due to liquefaction, *Soils and Foundations*, **32**(1), 149–160.
21) Youd, T. L. and Bartlett, S. F. (1988): US case histories of liquefaction-induced ground displacement, *Proc. 1st JAPAN-U.S. Workshop on Liquefaction, Large Ground Deformation and Their Effects on Lifeline Facilities*, 22–31.